Remote Entanglement via Adiabatic Passage Using a Tunably Dissipative Quantum Communication System

H.-S. Chang,[1] Y. P. Zhong,[1] A. Bienfait,[1,†] M.-H. Chou,[1,2] C. R. Conner,[1] É. Dumur,[1,3,‡] J. Grebel,[1] G. A. Peairs,[4,1] R. G. Povey,[1,2] K. J. Satzinger,[4,1,§] and A. N. Cleland[1,3,*]

[1]Pritzker School of Molecular Engineering, University of Chicago, Chicago, Illinois 60637, USA
[2]Department of Physics, University of Chicago, Chicago, Illinois 60637, USA
[3]Argonne National Laboratory, Argonne, Illinois 60439, USA
[4]Department of Physics, University of California, Santa Barbara, California 93106, USA

(Received 2 April 2020; accepted 18 May 2020; published 17 June 2020)

Effective quantum communication between remote quantum nodes requires high fidelity quantum state transfer and remote entanglement generation. Recent experiments have demonstrated that microwave photons, as well as phonons, can be used to couple superconducting qubits, with a fidelity limited primarily by loss in the communication channel [P. Kurpiers *et al.*, Nature (London) **558**, 264 (2018); C. J. Axline *et al.*, Nat. Phys. **14**, 705 (2018); P. Campagne-Ibarcq *et al.*, Phys. Rev. Lett. **120**, 200501 (2018); N. Leung *et al.*, npj Quantum Inf. **5**, 18 (2019); Y. P. Zhong *et al.*, Nat. Phys. **15**, 741 (2019); A. Bienfait *et al.*, Science **364**, 368 (2019)]. Adiabatic protocols can overcome channel loss by transferring quantum states without populating the lossy communication channel. Here, we present a unique superconducting quantum communication system, comprising two superconducting qubits connected by a 0.73 m-long communication channel. Significantly, we can introduce large tunable loss to the channel, allowing exploration of different entanglement protocols in the presence of dissipation. When set for minimum loss in the channel, we demonstrate an adiabatic quantum state transfer protocol that achieves 99% transfer efficiency as well as the deterministic generation of entangled Bell states with a fidelity of 96%, all without populating the intervening communication channel, and competitive with a qubit-resonant mode-qubit relay method. We also explore the performance of the adiabatic protocol in the presence of significant channel loss, and show that the adiabatic protocol protects against loss in the channel, achieving higher state transfer and entanglement fidelities than the relay method.

DOI: 10.1103/PhysRevLett.124.240502

Remote entanglement of superconducting qubits has recently been demonstrated using both microwave photon- and phonon-mediated communication [1–6]. Many of these demonstrations are limited by loss in the communication channel, due to loss in the various microwave components or intrinsic to the channel itself [1,4,6]; similar limitations apply to, e.g., optically based quantum communication systems. Adiabatic protocols analogous to stimulated Raman adiabatic passage [7,8] can mitigate such loss by adiabatically evolving an eigenstate of the system, using states that are "dark" with respect to the communication channel. These enable the high-fidelity coherent transfer of quantum states between sender and receiver nodes, even in the presence of large channel loss. Despite their use in a number of localized systems, such protocols have not been used for the generation of remote entangled states [7,8].

In this Letter, we present a unique experimental system comprising a pair of superconducting transmon-style qubits linked by an on-chip, 0.73 m-long superconducting microwave transmission line. By changing the coupling of the transmission line to a resistive load, we can vary the energy lifetime T_{1r} of the transmission line over 2 orders of magnitude. We demonstrate an adiabatic protocol for quantum communication between the qubit nodes, compare its performance to a qubit-transmission mode-qubit relay method [5,9,10], and explore the performance of both protocols as a function of transmission loss.

First, we describe the experimental device, then the two-state transfer methods. We test the performance of each protocol in the low-loss limit, then as a function of transmission loss. The adiabatic process achieves significantly improved performance compared to the relay method, especially at intermediate levels of loss in the channel.

The two quantum state transfer methods, and the device we use to test them, are shown in Fig. 1. The device comprises two frequency-tunable superconducting Xmon qubits [11,12], Q_1 and Q_2, each coupled to one end of the on-chip transmission line via an electrically controlled tunable coupler [13], G_1 and G_2, respectively [Fig. 1(b)]. We use the qubit ground $|g\rangle$ and excited $|e\rangle$ states, whose transition frequency is tunable from ~3 to 6 GHz. Qubit control is via low-frequency flux tuning for Z control and quadrature-resolved microwave pulses for XY control. We read out the qubit states using standard dispersive measurements [14–16],

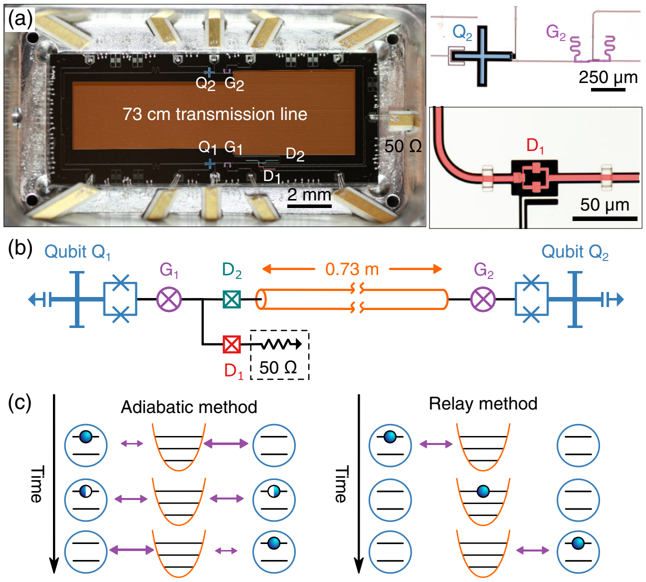

FIG. 1. Experimental device. (a) Optical micrograph of the device (left), with magnified views of one qubit and its associated tunable coupler (right top), and one variable loss coupler (right bottom). (b) A simplified circuit schematic, with two superconducting qubits (Q_1 and Q_2, blue), coupled by tunable couplers (G_1 and G_2, purple) to a 0.73 m-long superconducting transmission line (orange). The transmission line is interrupted near Q_1 by a tunable switch. The switch comprises two tunable couplers D_1 (red) and D_2 (teal), with D_1 connected to an external 50 Ω load to ground (dashed box), while D_2 connects to the remainder of the transmission line. Complete circuit diagram and parameters are provided in [17].

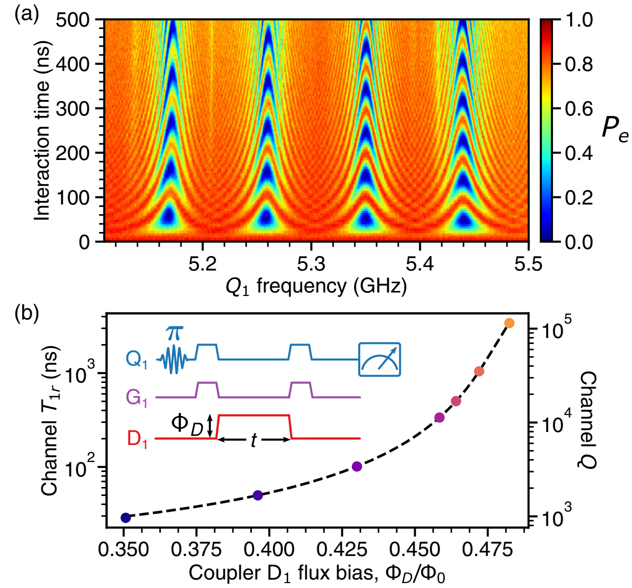

FIG. 2. Variable loss transmission channel. (a) Vacuum Rabi swaps between qubit Q_1 and four sequential resonant transmission line modes. The coupling is set to $|g_1|/2\pi = 5.0 \pm 0.1$ MHz $\ll \omega_{\mathrm{FSR}}/2\pi$. (b) Measurement of the energy lifetime T_{1r} of one resonant mode in the transmission line, at 5.351 GHz, with equivalent quality factors Q shown on right; inset shows pulse sequence. A π pulse to qubit Q_1 puts it in the excited state, and this excitation is swapped into the resonant mode for a time t, after which it is recovered and the qubit P_e measured. The corresponding lifetime is measured as a function of transmission line loss, controlled during the lifetime measurement using coupler D_1. With D_1 turned off, we find the intrinsic lifetime $T_{1r} = 3410 \pm 40$ ns (orange); with maximum loss, we find $T_{1r} = 28.7 \pm 0.2$ ns (blue). The standard deviation of each data point is smaller than the points. Dashed lines are results calculated with a circuit model; see [17].

via a capacitively coupled readout resonator and a traveling-wave parametric amplifier. We projectively measure the excited state probability P_e of each qubit with a fidelity of $88.8 \pm 0.8\%$.

The tunable couplers G_1 and G_2 allow us to externally control the coupling $g_{1,2}$ of each qubit to the individual resonant modes in the transmission line. A variable control consisting of two additional tunable couplers, D_1 and D_2, is integrated into the transmission line, 1.6 mm from the coupler G_1 and its associated qubit Q_1. This circuit element provides electrically controlled coupling between its input port and two output ports [36]. The coupler D_2 is placed inline with the transmission line and is always set to provide maximum coupling (and minimal reflection) to the remaining length of the transmission line. The other coupler D_1 connects to port 1 on the sample mount, which is terminated by a lumped 50Ω microwave load outside the sample box. Varying the coupling to this load allows us to set the loss in the transmission line, quantified by the energy lifetime T_{1r} of each resonant mode.

The transmission line of length $\ell = 0.73$ m supports multiple resonant modes, separated in frequency by the free spectral range (FSR) $\omega_{\mathrm{FSR}}/2\pi = 1/2T_\ell = 84$ MHz, where $T_\ell = 5.9$ ns is the photon one-way transit time in the channel. For a sufficiently small qubit-resonator coupling, $g_{1,2} \ll \omega_{\mathrm{FSR}}$, each qubit can be selectively coupled to a single resonant mode in the transmission line. This is shown in Fig. 2(a), where the transition frequency $\omega_{ge}/2\pi$ of qubit Q_1 is tuned over 400 MHz, yielding four separate vacuum Rabi swap resonances spaced by the free spectral range $\omega_{\mathrm{FSR}}/2\pi$. The loss coupler D_1 was set to minimum coupling, so the transmission line is limited only by its intrinsic loss. All experiments, here, were done with the mode at 5.351 GHz, just to the right of center in Fig. 2(a).

In Fig. 2(b), we demonstrate tunable control over the channel loss, using qubit Q_1 to measure the lifetime of the resonant mode at 5.531 GHz as we vary the coupler D_1 and, thus, the transmission line loss. The pulse sequence for this measurement is shown in the inset in Fig. 2(b). The mode energy decay time T_{1r} for each loss setting (controlled by the D_1 flux) is shown in Fig. 2(b). With no coupling through D_1, we measure the intrinsic resonant mode lifetime $T_{1r} \approx 3410 \pm 40$ ns (orange), comparable to similar transmission lines without variable loss [5].

With maximum coupling to the load, we measure a lifetime $T_{1r} \approx 28.7 \pm 0.2$ ns (blue), corresponding to a loaded quality factor $Q_r = 960$, about 120 times smaller than the intrinsic quality factor of 1.1×10^5. We also measure the resonant mode's Ramsey dephasing time T_{2r} at various D_1 flux bias points and find $T_{2r} \approx 2T_{1r}$, indicating the coupler D_1 introduces negligible additional phase decoherence. One nonideality with this system is that qubit Q_1, due to its close proximity to the loss coupler D_1, also has its lifetime reduced when the couplers G_1 and D_1 are both set to nonzero coupling, allowing energy loss from Q_1 to the external load; this limits the performance of Q_1 and is discussed further in the Supplemental Material [17–36]. This additional loss pathway could be reduced by placing the loss coupler D_1 in the center of the transmission line, as the transmission line would then protect both qubits from the external load.

We used two different communication protocols, adiabatic transfer and a qubit-resonant mode-qubit relay method. Both methods were used for qubit state transfer via the transmission line as well as Bell state generation, both as a function of loss in the communication channel. The relay method uses a single extended mode in the transmission line, swapping an excitation from one qubit into that mode and subsequently swapping the excitation from that mode to the other qubit. This method is described in detail elsewhere [5]; here, it achieves an intrinsic loss-limited state transfer efficiency of $\eta = 0.95 \pm 0.01$ and a Bell state fidelity of $\mathcal{F}_s = \langle \psi^- | \rho | \psi^- \rangle = 0.941 \pm 0.005$, where ρ is the measured density matrix and $|\psi^-\rangle = (|eg\rangle - |ge\rangle)/\sqrt{2}$ is the reference Bell singlet state.

The adiabatic method uses the variable coupling of each qubit to the transmission line. When qubits Q_1 and Q_2 are set to the same frequency and couple to the same resonant mode in the channel with strengths $g_1(t)$ and $g_2(t)$, the single-excitation Hamiltonian for the system can be written in the rotating frame as

$$H/\hbar = g_1(t)(|e0g\rangle\langle g1g| + |g1g\rangle\langle e0g|) + g_2(t)(|g0e\rangle\langle g1g| + |g1g\rangle\langle g0e|), \qquad (1)$$

where $|aNb\rangle$ corresponds to Q_1 (Q_2) in $|a\rangle$ ($|b\rangle$) with N photons in the resonant transmission line mode. This Hamiltonian supports a dark eigenstate $|D\rangle$ that has no occupancy in the resonant mode,

$$|D(t)\rangle = \frac{1}{\sqrt{2}}[\cos\theta(t)|e0g\rangle - \sin\theta(t)|g0e\rangle], \qquad (2)$$

where the mixing angle θ is given by $\tan\theta(t) = g_1(t)/g_2(t)$. With g_1 set to zero and g_2 to its maximum, the dark state is $|D\rangle = |e0g\rangle$, while exchanging the coupling values $g_1 \leftrightarrow g_2$ yields the dark state $|g0e\rangle$. By adiabatically varying the ratio $g_1(t)/g_2(t)$ in time from zero to its maximum, the system will swap the excitation from Q_1 to Q_2, without populating the lossy intermediate channel [7,37].

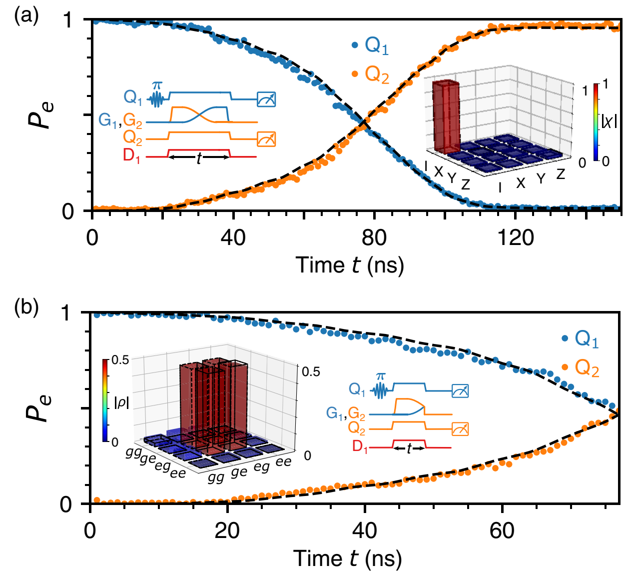

FIG. 3. Quantum state transfer and remote entanglement using the adiabatic protocol. (a) Adiabatic state transfer between qubits Q_1 and Q_2, measured with intrinsic loss in the transmission line. Blue (orange) circles represent excited state populations of Q_1 (Q_2) measured simultaneously at time t. Left inset: Control pulse sequence. The couplers are set so that coupling g_2 starts at its maximum with g_1 set to zero. Dissipation in the resonant channel mode is controlled using D_1, here, set to zero coupling. Right inset: Quantum process tomography, yielding a process fidelity $\mathcal{F}_p = 0.96 \pm 0.01$. (b) Adiabatic remote entanglement. Right inset shows control pulse sequence: With Q_1 initially prepared in $|e\rangle$, G_1 and G_2 are controlled using the adiabatic protocol to share half of Q_1's excitation with Q_2, resulting in a Bell singlet state $|\psi^-\rangle = (|eg\rangle - |ge\rangle)/\sqrt{2}$. Blue (orange) circles represent excited state populations of Q_1 (Q_2) measured simultaneously at time t. Left inset: Reconstructed density matrix of the final Bell state, yielding a state fidelity $\mathcal{F}_s = 0.964 \pm 0.007$ and concurrence $\mathcal{C} = 0.95 \pm 0.01$. In all panels, dashed lines are from master equation simulations accounting for channel dissipation and qubit imperfections (see [17]).

Here, we implement a simple adiabatic scheme [37,38], where we vary the couplings in time according to $g_1(t) = \bar{g}\sin(\pi t/2t_f)$ and $g_2(t) = \bar{g}\cos(\pi t/2t_f)$. We choose the parameters $\bar{g}/2\pi = 15$ MHz and $t_f = 132$ ns, minimizing the impact of finite qubit coherence while maintaining sufficient adiabaticity (see [17]). We note that the adiabatic protocol supports better than 90% transfer efficiency even when $\bar{g} = 0.4\omega_{\rm FSR}$; see [17].

In Fig. 3(a), we demonstrate deterministic adiabatic state transfer from Q_1 to Q_2. With Q_1 in $|e\rangle$ and Q_1 and Q_2 set on resonance with a single mode in the channel, we adjust the couplers G_1 and G_2 adiabatically to complete the state transfer. We show the excited state population of each qubit as a function of time t, measured with the resonant mode loss at its intrinsic minimum. We observe the expected gradual population transfer from Q_1 to Q_2, with the population of Q_2 reaching its maximum at $t = t_f$, with a transfer efficiency $\eta = P_{e,Q_2}(t = t_f)/P_{e,Q_1}(t = 0) = 0.99 \pm 0.01$. We further characterize the state transfer by carrying out quantum process tomography [39], yielding the process matrix χ shown in the inset in Fig. 3(a), with a process fidelity $\mathcal{F}_p = 0.96 \pm 0.01$, limited by qubit decoherence. The process matrix calculated from a master equation simulation displays a small trace distance to the measured χ matrix of $\mathcal{D} = \sqrt{\mathrm{Tr}([\chi - \chi_{\mathrm{sim}}]^2)} = 0.02 \pm 0.01$, indicating excellent agreement with experiment.

The adiabatic protocol can also be used to generate remote entanglement between Q_1 and Q_2. With Q_1 prepared in $|e\rangle$, we share half its excitation with Q_2 using the adiabatic protocol, by stopping the transfer at its midpoint $t = t_f/2$. This generates a Bell singlet state $|\psi^-\rangle = (|eg\rangle - |ge\rangle)/\sqrt{2}$. The qubit excited state population is shown as a function of time t in Fig. 3(b). We further characterize the Bell state by quantum state tomography [40,41], and the reconstructed density matrix ρ is shown in the inset in Fig. 3(b). We find a Bell state fidelity $\mathcal{F}_s = \langle\psi^-|\rho|\psi^-\rangle = 0.964 \pm 0.007$, referenced to the ideal Bell singlet state ψ^-, and a concurrence $\mathcal{C} = 0.95 \pm 0.01$ (see [17]). The density matrix ρ_{sim} calculated from a master equation simulation shows a small trace distance to the measured ρ, $\sqrt{\mathrm{Tr}(|\rho - \rho_{\mathrm{sim}}|^2)} = 0.01$, indicating excellent agreement with experiment.

We explore the impact of loss on both the relay method and the adiabatic protocol, with results shown as a function of the resonant channel mode energy lifetime T_{1r} in Fig 4. For the highest level of dissipation, with $T_{1r} = 28.7$ ns, we measure an adiabatic transfer efficiency $\eta = 0.67 \pm 0.01$, even though the transfer time t_f is four times the resonant mode lifetime. The efficiency is primarily limited by loss in qubit Q_1 due to its spurious coupling loss through D_1 to the 50 Ω load (see [17]), in good agreement with master equation simulations. Results from a simulation without the spurious coupling are plotted as black dashed lines in Fig 4(a), limited by a small channel occupation due to the finite adiabaticity of the sequence. We compare these results to the relay method, where we use a weak coupling $|g_{1,2}|/2\pi = 5.0$ MHz to ensure that the qubits only couple to a single transmission line mode; this results in a total transfer time $2\tau_{\mathrm{swap}} = 100$ ns. We find the adiabatic protocol consistently performs better than the relay method, with a 2.6× higher transfer efficiency η (2.3× reduction in transfer loss) and 1.5× higher process fidelity $\mathcal{F}_p$ (2.3× reduction in process infidelity) compared to the relay method in the most dissipative case; the adiabatic protocol is primarily limited by spurious coupling loss in Q_1, while the relay method is limited by loss in the channel (see [17]).

In Fig. 4(b), we display the entanglement fidelity using the adiabatic protocol with different levels of channel loss, and compare to the relay method. The adiabatic protocol outperforms the relay method in all levels of dissipation. At the highest loss level, where $T_{1r} = 28.7$ ns, the adiabatic protocol achieves 1.2× higher Bell state fidelity $\mathcal{F}_s$ (1.5× reduction in Bell state infidelity) and 1.3× higher concurrence $\mathcal{C}$ (1.7× reduction in concurrence infidelity) compared to the relay method; the spurious-coupling-free simulation result for the adiabatic protocol is shown by the black dashed lines, limited by a small channel occupation due to the finite adiabaticity of the sequence.

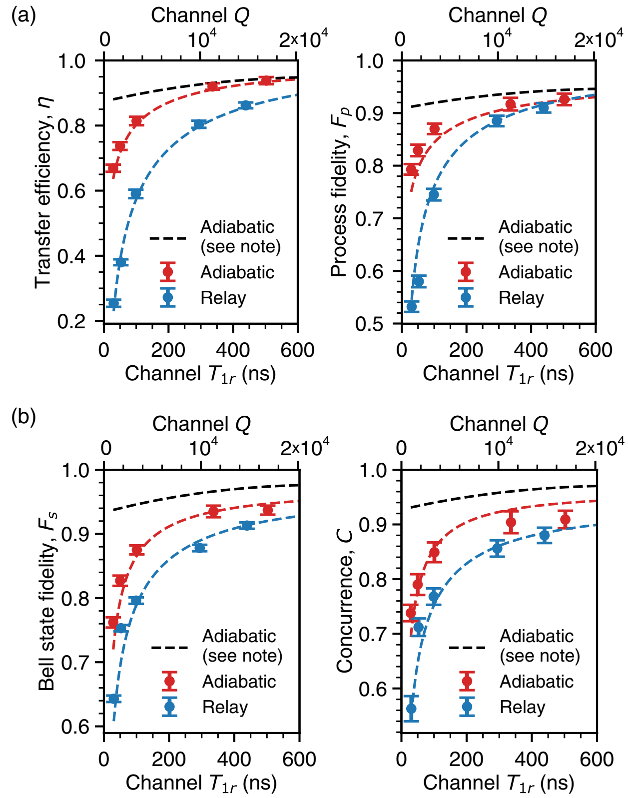

FIG. 4. Quantum communication in the presence of channel loss, using both the relay method and adiabatic protocol. (a) Measured transfer efficiency η (left) and process fidelity $\mathcal{F}_p$ (right) for the adiabatic protocol (red) and the relay method (blue), for different resonant channel mode lifetimes T_{1r}, with equivalent quality factors Q shown on top. (b) Measured Bell state fidelity $\mathcal{F}_s$ (left) and concurrence $\mathcal{C}$ (right) for adiabatic protocol (red) and relay method (blue). In all panels, error bars are 1 standard deviation; red and blue dashed lines are from simulations including all sources of loss, and black dashed lines are from a master equation simulation for the adiabatic protocol with no Q_1 spurious coupling loss (see [17]).

In conclusion, we describe a unique experimental system in which we can explore the performance of quantum communication protocols in the presence of controllable communication loss. We demonstrate an adiabatic protocol that realizes high-fidelity transfer of quantum states and entangled Bell states, limited mostly by spurious coupling of one qubit to the controlled transmission line loss. The platform we have developed is well-suited for exploring the impact of channel loss on other error-protecting quantum communication protocols, such as heralding [42–44] and entanglement distillation [45–47]. The ability to introduce controlled loss dynamically into the system opens the door for studying dissipative dynamics in nonequilibrium systems, enabling approaches such as reservoir engineering [48,49]. The adiabatic protocol demonstrated here is applicable to other quantum communication systems, for example, phonon-based systems where the communication channel is significantly more lossy [6,50,51]. Future demonstrations could employ more advanced adiabatic protocols such as shortcuts to adiabaticity [52,53] and composite adiabatic passage [54,55] to further improve fidelity.

The authors declare no competing financial interests.

The authors thank A. A. Clerk, P. J. Duda, and B. B. Zhou for helpful discussions. We thank W. D. Oliver and G. Calusine at MIT Lincoln Lab for providing the traveling-wave parametric amplifier (TWPA) used in this work. Devices and experiments were supported by the Air Force Office of Scientific Research and the Army Research Laboratory. K. J. S. was supported by NSF GRFP (NSF Grant No. DGE-1144085), É. D. was supported by LDRD funds from Argonne National Laboratory; A. N. C. was supported in part by the DOE, Office of Basic Energy Sciences. This work was partially supported by the UChicago MRSEC (NSF Grant No. DMR-1420709) and made use of the Pritzker Nanofabrication Facility, which receives support from SHyNE, a node of the National Science Foundation's National Nanotechnology Coordinated Infrastructure (NSF Grant No. NNCI-1542205). Correspondence and requests for materials should be addressed to A. N. Cleland (anc@uchicago.edu).

[*]Corresponding author.
anc@uchicago.edu

[†]Present address: Université de Lyon, ENS de Lyon, Université Claude Bernard, CNRS, Laboratoire de Physique, F-69342 Lyon, France.

[‡]Present address: Université Grenoble Alpes, CEA, INAC-Pheliqs, 38000 Grenoble, France.

[§]Present address: Google, Santa Barbara, California 93117, USA.

[1] P. Kurpiers, P. Magnard, T. Walter, B. Royer, M. Pechal, J. Heinsoo, Y. Salathe, A. Akin, S. Storz, J.-C. Besse, S. Gasparinetti, A. Blais, and A. Wallraff, Deterministic quantum state transfer and remote entanglement using microwave photons, Nature (London) **558**, 264 (2018).

[2] C. J. Axline, L. D. Burkhart, W. Pfaff, M. Zhang, K. Chou, P. Campagne-Ibarcq, P. Reinhold, L. Frunzio, S. M. Girvin, L. Jiang, M. H. Devoret, and R. J. Schoelkopf, On-demand quantum state transfer and entanglement between remote microwave cavity memories, Nat. Phys. **14**, 705 (2018).

[3] P. Campagne-Ibarcq, E. Zalys-Geller, A. Narla, S. Shankar, P. Reinhold, L. Burkhart, C. Axline, W. Pfaff, L. Frunzio, R. J. Schoelkopf, and M. H. Devoret, Deterministic Remote Entanglement of Superconducting Circuits through Microwave Two-Photon Transitions, Phys. Rev. Lett. **120**, 200501 (2018).

[4] N. Leung, Y. Lu, S. Chakram, R. K. Naik, N. Earnest, R. Ma, K. Jacobs, A. N. Cleland, and D. I. Schuster, Deterministic bidirectional communication and remote entanglement generation between superconducting qubits, npj Quantum Inf. **5**, 18 (2019).

[5] Y. P. Zhong, H.-S. Chang, K. J. Satzinger, M.-H. Chou, A. Bienfait, C. R. Conner, É. Dumur, J. Grebel, G. A. Peairs, R. G. Povey, D. I. Schuster, and A. N. Cleland, Violating Bell's inequality with remotely connected superconducting qubits, Nat. Phys. **15**, 741 (2019).

[6] A. Bienfait, K. J. Satzinger, Y. P. Zhong, H.-S. Chang, M.-H. Chou, C. R. Conner, É. Dumur, J. Grebel, G. A. Peairs, R. G. Povey, and A. N. Cleland, Phonon-mediated quantum state transfer and remote qubit entanglement, Science **364**, 368 (2019).

[7] N. V. Vitanov, A. A. Rangelov, B. W. Shore, and K. Bergmann, Stimulated Raman adiabatic passage in physics, chemistry, and beyond, Rev. Mod. Phys. **89**, 015006 (2017).

[8] K. Bergmann *et al.*, Roadmap on STIRAP applications, J. Phys. B **52**, 202001 (2019).

[9] M. A. Sillanpaa, J. I. Park, and R. W. Simmonds, Coherent quantum state storage and transfer between two phase qubits via a resonant cavity, Nature (London) **449**, 438 (2007).

[10] M. Ansmann, H. Wang, R. C. Bialczak, M. Hofheinz, E. Lucero, M. Neeley, A. D. O'Connell, D. Sank, M. Weides, J. Wenner, A. N. Cleland, and J. M. Martinis, Violation of Bell's inequality in Josephson phase qubits, Nature (London) **461**, 504 (2009).

[11] J. Koch, T. M. Yu, J. Gambetta, A. A. Houck, D. I. Schuster, J. Majer, A. Blais, M. H. Devoret, S. M. Girvin, and R. J. Schoelkopf, Charge-insensitive qubit design derived from the Cooper pair box, Phys. Rev. A **76**, 042319 (2007).

[12] R. Barends, J. Kelly, A. Megrant, D. Sank, E. Jeffrey, Y. Chen, Y. Yin, B. Chiaro, J. Mutus, C. Neill, P. O'Malley, P. Roushan, J. Wenner, T. C. White, A. N. Cleland, and J. M. Martinis, Coherent Josephson Qubit Suitable for Scalable Quantum Integrated Circuits, Phys. Rev. Lett. **111**, 080502 (2013).

[13] Y. Chen *et al.*, Qubit Architecture with High Coherence and Fast Tunable Coupling, Phys. Rev. Lett. **113**, 220502 (2014).

[14] D. I. Schuster, A. Wallraff, A. Blais, L. Frunzio, R.-S. Huang, J. Majer, S. M. Girvin, and R. J. Schoelkopf, ac Stark Shift and Dephasing of a Superconducting Qubit Strongly Coupled to a Cavity Field, Phys. Rev. Lett. **94**, 123602 (2005).

[15] A. Wallraff, D. I. Schuster, A. Blais, L. Frunzio, J. Majer, M. H. Devoret, S. M. Girvin, and R. J. Schoelkopf, Approaching Unit Visibility for Control of a Superconducting Qubit with Dispersive Readout, Phys. Rev. Lett. **95**, 060501 (2005).

[16] A. Blais, R.-S. Huang, A. Wallraff, S. M. Girvin, and R. J. Schoelkopf, Cavity quantum electrodynamics for superconducting electrical circuits: An architecture for quantum computation, Phys. Rev. A **69**, 062320 (2004).

[17] See Supplemental Material at http://link.aps.org/supplemental/10.1103/PhysRevLett.124.240502 for further experimental details and data analysis, as well as for Refs. [18–35].

[18] E. Jeffrey, D. Sank, J. Y. Mutus, T. C. White, J. Kelly, R. Barends, Y. Chen, Z. Chen, B. Chiaro, A. Dunsworth, A. Megrant, P. J. J. O'Malley, C. Neill, P. Roushan, A. Vainsencher, J. Wenner, A. N. Cleland, and J. M. Martinis, Fast Accurate State Measurement with Superconducting Qubits, Phys. Rev. Lett. **112**, 190504 (2014).

[19] J. Kelly *et al.*, State preservation by repetitive error detection in a superconducting quantum circuit, Nature (London) **519**, 66 (2015).

[20] C. Macklin, K. O'Brien, D. Hover, M. E. Schwartz, V. Bolkhovsky, X. Zhang, W. D. Oliver, and I. Siddiqi, A near-quantum-limited Josephson traveling-wave parametric amplifier, Science **350**, 307 (2015).

[21] D. M. Pozar, *Microwave Engineering*, 4th ed. (Wiley, Hoboken, NJ, 2012).

[22] J. M. Chow, L. DiCarlo, J. M. Gambetta, A. Nunnenkamp, L. S. Bishop, L. Frunzio, M. H. Devoret, S. M. Girvin, and R. J. Schoelkopf, Detecting highly entangled states with a joint qubit readout, Phys. Rev. A **81**, 062325 (2010).

[23] H. K. Xu, C. Song, W. Y. Liu, G. M. Xue, F. F. Su, H. Deng, Y. Tian, D. N. Zheng, S. Han, Y. P. Zhong, H. Wang, Y.-x. Liu, and S. P. Zhao, Coherent population transfer between uncoupled or weakly coupled states in ladder-type superconducting qutrits, Nat. Commun. **7**, 11018 (2016).

[24] K. Bergmann, H. Theuer, and B. W. Shore, Coherent population transfer among quantum states of atoms and molecules, Rev. Mod. Phys. **70**, 1003 (1998).

[25] B. W. Shore, *Manipulating Quantum Structures Using Laser Pulses* (Cambridge University Press, Cambridge, England, New York, 2011).

[26] M. O. Scully and M. S. Zubairy, *Quantum Optics* (Cambridge University Press, Cambridge, England, 1997).

[27] G. S. Vasilev, A. Kuhn, and N. V. Vitanov, Optimum pulse shapes for stimulated Raman adiabatic passage, Phys. Rev. A **80**, 013417 (2009).

[28] S. Guerin, S. Thomas, and H. R. Jauslin, Optimization of population transfer by adiabatic passage, Phys. Rev. A **65**, 023409 (2002).

[29] T. Pellizzari, Quantum Networking with Optical Fibers, Phys. Rev. Lett. **79**, 5242 (1997).

[30] B. Vogell, B. Vermersch, T. E. Northup, B. P. Lanyon, and C. A. Muschik, Deterministic quantum state transfer between remote qubits in cavities, Quantum Sci. Technol. **2**, 045003 (2017).

[31] G. Lindblad, On the generators of quantum dynamical semigroups, Commun. Math. Phys. **48**, 119 (1976).

[32] D. F. Walls and G. J. Milburn, *Quantum Optics*, 2nd ed. (Springer, Berlin, 2008).

[33] J. Johansson, P. Nation, and F. Nori, QuTiP: An open-source Python framework for the dynamics of open quantum systems, Comput. Phys. Commun. **183**, 1760 (2012).

[34] W. K. Wootters, Entanglement of Formation of an Arbitrary State of Two Qubits, Phys. Rev. Lett. **80**, 2245 (1998).

[35] M. B. Plenio and S. Virmani, An introduction to entanglement measures, Quantum Inf. Comput. **7**, 1 (2007).

[36] H.-S. Chang, Y. P. Zhong, K. J. Satzinger, M.-H. Chou, A. Bienfait, C. R. Conner, É. Dumur, J. Grebel, G. A. Peairs, R. G. Povey, and A. N. Cleland (to be published).

[37] Y.-D. Wang and A. A. Clerk, Using dark modes for high-fidelity optomechanical quantum state transfer, New J. Phys. **14**, 105010 (2012).

[38] Y.-D. Wang, R. Zhang, X.-B. Yan, and S. Chesi, Optimization of STIRAP-based state transfer under dissipation, New J. Phys. **19**, 093016 (2017).

[39] M. Neeley, M. Ansmann, R. C. Bialczak, M. Hofheinz, N. Katz, E. Lucero, A. O'Connell, H. Wang, A. N. Cleland, and J. M. Martinis, Process tomography of quantum memory in a Josephson-phase qubit coupled to a two-level state, Nat. Phys. **4**, 523 (2008).

[40] M. Steffen, M. Ansmann, R. C. Bialczak, N. Katz, E. Lucero, R. McDermott, M. Neeley, E. M. Weig, A. N. Cleland, and J. M. Martinis, Measurement of the entanglement of two superconducting qubits via state tomography, Science **313**, 1423 (2006).

[41] M. Neeley, R. C. Bialczak, M. Lenander, E. Lucero, M. Mariantoni, A. D. O'Connell, D. Sank, H. Wang, M. Weides, J. Wenner, Y. Yin, T. Yamamoto, A. N. Cleland, and J. M. Martinis, Generation of three-qubit entangled states using superconducting phase qubits, Nature (London) **467**, 570 (2010).

[42] P. J. Mosley, J. S. Lundeen, B. J. Smith, P. Wasylczyk, A. B. U'Ren, C. Silberhorn, and I. A. Walmsley, Heralded Generation of Ultrafast Single Photons in Pure Quantum States, Phys. Rev. Lett. **100**, 133601 (2008).

[43] K. Azuma, K. Tamaki, and H.-K. Lo, All-photonic quantum repeaters, Nat. Commun. **6**, 6787 (2015).

[44] P. Kurpiers, M. Pechal, B. Royer, P. Magnard, T. Walter, J. Heinsoo, Y. Salathe, A. Akin, S. Storz, J.-C. Besse, S. Gasparinetti, A. Blais, and A. Wallraff, Quantum Communication with Time-Bin Encoded Microwave Photons, Phys. Rev. Applied **12**, 044067 (2019).

[45] P. G. Kwiat, S. Barraza-Lopez, A. Stefanov, and N. Gisin, Experimental entanglement distillation and hidden non-locality, Nature (London) **409**, 1014 (2001).

[46] R. Dong, M. Lassen, J. Heersink, C. Marquardt, R. Filip, G. Leuchs, and U. L. Andersen, Experimental entanglement distillation of mesoscopic quantum states, Nat. Phys. **4**, 919 (2008).

[47] H. Takahashi, J. S. Neergaard-Nielsen, M. Takeuchi, M. Takeoka, K. Hayasaka, A. Furusawa, and M. Sasaki, Entanglement distillation from Gaussian input states, Nat. Photonics **4**, 178 (2010).

[48] J. F. Poyatos, J. I. Cirac, and P. Zoller, Quantum Reservoir Engineering with Laser-Cooled Trapped Ions, Phys. Rev. Lett. **77**, 4728 (1996).

[49] M. B. Plenio and S. F. Huelga, Entangled Light from White Noise, Phys. Rev. Lett. **88**, 197901 (2002).

[50] S. Hermelin, S. Takada, M. Yamamoto, S. Tarucha, A. D. Wieck, L. Saminadayar, C. Bauerle, and T. Meunier, Electrons surfing on a sound wave as a platform for quantum optics with flying electrons, Nature (London) **477**, 435 (2011).

[51] R. P. G. McNeil, M. Kataoka, C. J. B. Ford, C. H. W. Barnes, D. Anderson, G. A. C. Jones, I. Farrer, and

D. A. Ritchie, On-demand single-electron transfer between distant quantum dots, Nature (London) **477**, 439 (2011).

[52] A. Baksic, H. Ribeiro, and A. A. Clerk, Speeding Up Adiabatic Quantum State Transfer by Using Dressed States, Phys. Rev. Lett. **116**, 230503 (2016).

[53] B. B. Zhou, A. Baksic, H. Ribeiro, C. G. Yale, F. J. Heremans, P. C. Jerger, A. Auer, G. Burkard, A. A. Clerk, and D. D. Awschalom, Accelerated quantum control using superadiabatic dynamics in a solid-state lambda system, Nat. Phys. **13**, 330 (2017).

[54] B. T. Torosov, S. Guerin, and N. V. Vitanov, High-Fidelity Adiabatic Passage by Composite Sequences of Chirped Pulses, Phys. Rev. Lett. **106**, 233001 (2011).

[55] A. Bruns, G. T. Genov, M. Hain, N. V. Vitanov, and T. Halfmann, Experimental demonstration of composite stimulated Raman adiabatic passage, Phys. Rev. A **98**, 053413 (2018).